Membrane Proteins

DOI: 10.1002/anie.201406603

Functional Dynamics of Deuterated β_2-Adrenergic Receptor in Lipid Bilayers Revealed by NMR Spectroscopy**

*Yutaka Kofuku, Takumi Ueda, Junya Okude, Yutaro Shiraishi, Keita Kondo, Takuya Mizumura, Shiho Suzuki, and Ichio Shimada**

Abstract: *G-protein-coupled receptors (GPCRs) exist in conformational equilibrium between active and inactive states, and the former population determines the efficacy of signaling. However, the conformational equilibrium of GPCRs in lipid bilayers is unknown owing to the low sensitivities of their NMR signals. To increase the signal intensities, a deuteration method was developed for GPCRs expressed in an insect cell/baculovirus expression system. The NMR sensitivities of the methionine methyl resonances from the β_2-adrenergic receptor (β_2AR) in lipid bilayers of reconstituted high-density lipoprotein (rHDL) increased by approximately 5-fold upon deuteration. NMR analyses revealed that the exchange rates for the conformational equilibrium of β_2AR in rHDLs were remarkably different from those measured in detergents. The timescales of GPCR signaling, calculated from the exchange rates, are faster than those of receptor tyrosine kinases and thus enable rapid neurotransmission and sensory perception.*

G-protein-coupled receptors (GPCRs) function as acceptors for various neurotransmitters, hormones, odorants, or tastants, and more than 30% of modern drugs target GPCRs.[1] The binding of these drugs to GPCRs leads to the activation or inhibition of intracellular G proteins and various other effectors. These GPCR signals are controlled with various strengths, as exemplified by the basal activity and partial agonism phenomena, and thus cannot be explained by simple transitions between inactive and active states. Our previous NMR study of the β_2-adrenergic receptor (β_2AR),[2] a class A GPCR that regulates various physiological events including bronchodilation, revealed that β_2AR exists in a conformational equilibrium between two inactive conformations and one active conformation, and that the population of the active conformation determines the signal strength. The conformational equilibrium of β_2AR was also observed in other NMR studies.[3] The conformational changes in the transmembrane (TM) region upon activation are broadly conserved among the class A GPCRs,[4] thus suggesting that other GPCRs also exist in conformational equilibrium as a general signature characteristic of GPCRs.

Whereas the β_2AR used in the previous NMR studies was solubilized by detergents, which are widely utilized for the structural investigation of membrane proteins, β_2AR is embedded in lipid bilayers under physiological conditions. It was recently reported that reconstituted high-density lipoproteins (rHDLs), which are also known as nanodiscs, can accommodate membrane proteins, including GPCRs, within a 10 nm-diameter disc-shaped lipid bilayer in a detergent-free solution.[5] CCR5, a member of the GPCR family, maintains its native conformation more stably in rHDLs than in detergent micelles.[5] Furthermore, GPCRs in rHDLs effectively activate G proteins that cannot be activated by GPCRs in detergent micelles, thus suggesting that rHDLs are better mimetics of the physiological lipid-bilayer environment than detergents.[5] NMR analyses of the deuterated potassium channel KcsA in rHDLs revealed that the populations of permeable and impermeable conformations were different from those measured in detergents,[6] thus suggesting that the conformational equilibria and functions of membrane proteins are affected by the lipid-bilayer environment. Therefore, the determination of the conformational dynamics of β_2AR under lipid-bilayer conditions is important for understanding its signal transduction mechanisms under physiological conditions.

Sensitivity enhancements by deuteration were required in the aforementioned NMR analyses of membrane proteins in rHDL.[7] However, it would be difficult to achieve deuteration for the previously observed NMR signals of the methionine methyl groups of β_2AR[2] because insect cells, which are utilized for the large-scale expression of functional β_2AR and various other eukaryotic proteins,[8] are unable to grow in minimal media,[9] and high concentrations of deuterium oxide are toxic to animal cells.[10]

In order to prepare deuterated and selectively methionine-labeled proteins by using the insect cell/baculovirus expression system, we added commercially available deuterated amino acids and algal amino acid mixtures, as well as [methyl-^{13}C]-methionine, to an amino acid deficient medium. Under optimized conditions (Table S1 in the Supporting Information), the ^{2}H and ^{13}C labeling efficiencies of each type of amino acid residue were calculated from NMR (Figures

[*] Dr. Y. Kofuku, Dr. T. Ueda, J. Okude, Y. Shiraishi, K. Kondo, T. Mizumura, S. Suzuki, Prof. Dr. I. Shimada
Graduate School of Pharmaceutical Sciences
The University of Tokyo
Hongo 7-3-1, Bunkyo-ku, Tokyo 113-0033 (Japan)
E-mail: shimada@iw-nmr.f.u-tokyo.ac.jp
Dr. T. Ueda
Precursory Research for Embryonic Science and Technology (PRESTO) (Japan) Science and Technology Agency (JST)
Chiyoda-ku, Tokyo 102-0075 (Japan)

[**] This work was supported in part by grants from the Japan New Energy and Industrial Technology Development Organization (NEDO) and the Ministry of Economy, Trade and Industry (METI), and by a Grant-in-Aid for Scientific Research on Priority Areas from the Japanese Ministry of Education, Culture, Sports, Science and Technology (MEXT).

Supporting information for this article is available on the WWW under http://dx.doi.org/10.1002/anie.201406603.

S1–S3 in the Supporting Information) and mass spectrometry analyses (Figure S4) of thioredoxin (Trx), which was used as a test case, as shown in Table S2 in the Supporting Information. Fourteen types of amino acid residue, which account for 88% of the GPCR TM residues, were deuterated (Figure S5).

In the case of insect cell/baculovirus expression of proteins with low yields, such as β_2AR, minimization of the number of deuterated amino acids is preferable because the protein yields are substantially reduced by the addition of deuterated amino acids to the medium. Therefore, we selected the deuterated amino acids based on the ^{1}H–^{1}H distances between the observed methionine methyl groups and each amino acid residue in the crystal structures of β_2AR, and the labeling efficiencies for Trx (Table S2). The deuterium incorporation rates for β_2AR are expected to be similar to those for Trx because the stable isotope incorporation rates in the insect cell/baculovirus expression system were determined by the populations of added labeled amino acids and residual nonlabeled amino acids in the medium.[8] Our calculations revealed that, in the case of the deuteration of alanine, cysteine, isoleucine, leucine, methionine, phenylalanine, threonine, valine, tyrosine, and tryptophan residues, the ^{1}H–^{1}H dipole–dipole interactions of the methyl groups of M82, M215, and M279, which are buried in the β_2AR TM region, would be 10–19% of those of nondeuterated β_2AR (Figure S6), and the sensitivities of the resonances from these residues would increase by about 3–7-fold upon deuteration. Hereafter, β_2AR obtained by this method is referred to as [^{2}H-9AA, αβγ-^{2}H-, methyl-^{13}C-Met] β_2AR. In order to observe the resonances from the methionine residues of β_2AR in rHDLs, we prepared [^{2}H-9AA, αβγ-^{2}H-, methyl-^{13}C-Met] β_2AR/4Met embedded in rHDLs (Figure S7 and Supporting Information). β_2AR/4Met possesses five methionine residues: M36, M40, M82, M215, and M279 (Figure S8a). M82, M215, and M279 assume distinctly different conformations between the crystal structures for β_2AR bound to an inverse agonist and β_2AR bound to a full agonist and G protein bound (Figure S8b),[11,12] and the resonances from these residues of the β_2AR 4Met mutant in DDM micelles exhibited large differences between each ligand-bound state.[2]

In the ^{1}H–^{13}C heteronuclear multiple quantum correlation (HMQC) spectrum of [^{2}H-9AA, αβγ-^{2}H-, methyl-^{13}C-Met] β_2AR/4Met in rHDLs in the bound state with the inverse agonist carazolol (Figure 1b), six resonances that correspond to all five methionine residues in β_2AR/4Met were observed, with the double peaks for M82. Assignments of the methionine resonances were established by comparison with the spectra of β_2AR or its mutants in micelles (Figures S9, S10, S11). In the spectra of β_2AR/4Met in rHDLs without deuteration (Figure 1a), the resonance from M36 was only observed with half the sensitivity of that of the deuterated β_2AR/4Met in rHDLs, and the M40, M82, M215, and M279 resonances were not clearly observed, thus suggesting that the sensitivities for these residues increased by more than 5-fold upon deuteration. These sensitivity enhancements are in agreement with the estimation from the decrease of the ^{1}H–^{1}H dipole–dipole interactions (Figure S6) that was calculated from the deuterium incorporation ratios of Trx (Table S2),

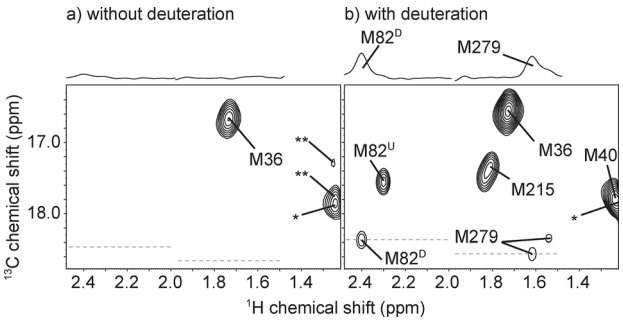

Figure 1. Sensitivity enhancements of the methionine resonances of β_2AR in rHDLs upon deuteration. ^{1}H–^{13}C HMQC spectra of [αβ-^{2}H-, methyl-^{13}C-Met] β_2AR/4Met in rHDLs (undeuterated; a) and [^{2}H-9AA, αβγ-^{2}H-, methyl-^{13}C-Met] β_2AR/4Met in rHDLs (deuterated; b) in the carazolol-bound state (see Figure S9 for details).

thus suggesting that the deuterium incorporation ratio of β_2AR was similar to that of Trx. In rHDLs, the M82 resonances of β_2AR, which is as large as 200 kDa, were clearly observed only in the spectra with deuteration (Figure 1), and thus deuteration was necessary to investigate the conformational dynamics of β_2AR in rHDLs by NMR.

In the bound state with the full agonist formoterol (Figure S12b), four resonances that correspond to M36, M40, M82, and M215 were observed. M279 was not clearly observed in the formoterol-bound state even under deuterated conditions, probably owing to severe exchange broadening. The chemical shifts of the resonances from M82 and M215 in the formoterol-bound state were remarkably different from those in the carazolol-bound state, whereas the resonances from M36 and M40 exhibited only small differences in chemical shift (Figure S12).

To investigate the effect of the lipid-bilayer environment on the equilibrium between the active and inactive conformations, ^{1}H–^{13}C HMQC spectra of [^{2}H-9AA, αβγ-^{2}H-, methyl-^{13}C-Met] β_2AR/4Met/M36L in rHDLs and in DDM micelles were recorded in the bound states with the neutral antagonist, alprenolol, and two partial agonists, tulobuterol and clenbuterol, and overlaid with the spectra for the bound states with carazolol and formoterol (Figure 2). The M36L mutation, which was introduced in order to overcome signal overlaps, does not affect the folding of β_2AR since the chemical shifts and signal intensities of the NMR resonances from M82, M215, and M279 did not exhibit notable changes with the M36L mutation in either the carazolol- or formoterol-bound states (Figure S13).

In the spectra of [^{2}H-9AA, αβγ-^{2}H-, methyl-^{13}C-Met] β_2AR/4Met/M36L in rHDLs and DDM micelles (Figure 2), two resonances from M82 with downfield and upfield chemical shifts, which were referred to as M82^D and M82^U, respectively, were observed in the carazolol-bound state, and one M82 resonance, which was referred to as M82^A, was observed in the formoterol-bound state, as in the previously reported spectra of nondeuterated 4Met mutant.[2] Furthermore, the M82 resonances from β_2AR bound to the neutral antagonist or partial agonists in rHDLs and in DDM micelles exhibited chemical shifts in an efficacy-dependent manner (Figure 2). As described previously,[2] these results suggest

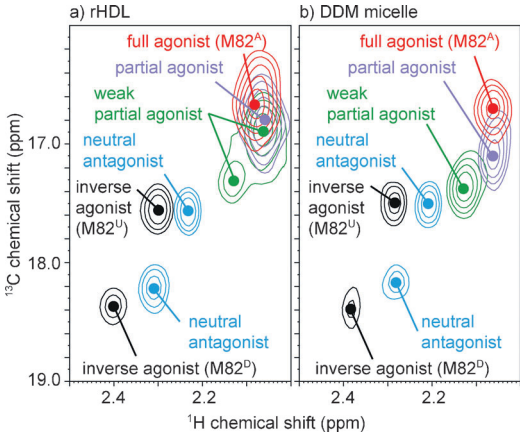

Figure 2. Differences in the M82 resonances of β_2AR with various ligands bound, in rHDLs and in DDM micelles. a) Overlaid ^{1}H–^{13}C HMQC spectra of [^{2}H-9AA, αβγ-^{2}H-, methyl-^{13}C-Met] β_2AR/4Met/M36L in rHDLs when bound to the inverse agonist carazolol (black), the neutral antagonist alprenolol (cyan), the weak partial agonist tulobuterol (green) the partial agonist clenbuterol (violet), or the full agonist formoterol (red). b) Overlaid ^{1}H–^{13}C HMQC spectra of [^{2}H-9AA, αβγ-^{2}H-, methyl-^{13}C-Met] β_2AR/4Met/M36L in DDM micelles, colored as in panel (a). In (a) and (b), only the regions with M82 resonances are shown, and the centers of the M82 resonances are indicated by dots.

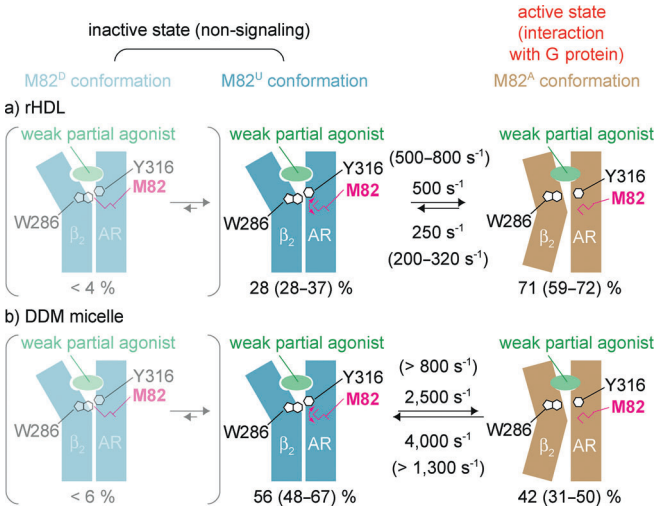

Figure 3. The differences in conformational equilibrium between β_2AR in rHDLs and β_2AR in DDM micelles. A proposed conformational equilibrium of β_2AR in rHDLs (a) or in DDM micelles (b) in the tulobuterol-bound state. Displayed populations and transition rates are the median, minimum, and maximum of the ensembles of the selected resonances in the simulation analyses (Figure S16). The states with populations less than 10% are displayed in a fainter color. See the Discussion in the Supporting Information for further details.

that β_2AR in rHDLs exists in an equilibrium between two inactive conformations (M82^D and M82^U conformations), which correspond to the crystal structures of β_2AR bound to inverse agonists,[11] and one active conformation (M82^A conformation), which corresponds to the crystal structure of β_2AR bound to a full agonist and a G-protein,[12] as is the case for β_2AR in DDM micelles.[2]

By contrast, the chemical shifts and lineshapes of the M82 resonances of β_2AR in rHDLs bound to the partial agonists were remarkably different from those for β_2AR in DDM micelles (Figure 2 and Figure S14). β_2AR bound to tulobuterol in rHDLs exhibited resonances with broad and complex lineshapes and chemical shifts between M82^U and M82^A, whereas β_2AR in DDM micelles exhibited one relatively intense signal (Figure 2 and Figure S14). These results suggest that the exchange rates between the M82^D, M82^U, and M82^A conformations of β_2AR in rHDLs are lower than those for β_2AR in DDM micelles. It is unlikely that the differences are due to direct interactions with lipids since M82 is completely buried in the TM region and cannot contact lipids or detergents. Furthermore, the M82 resonances of β_2AR bound to tulobuterol and clenbuterol in rHDLs were shifted toward M82^A (Figure 2 and Figure S14) in comparison to those of β_2AR in DDM micelles, thus suggesting that the population of the M82^A conformation of β_2AR in rHDLs is higher than in DDM micelles. Based on one-dimensional simulations of the M82 resonances in each ligand-bound state of β_2AR (Figures S15, S16, and Discussion in the Supporting Information), we concluded that the exchange rates between the active and inactive conformations were lower in rHDLs than in DDM micelles, and that the population of the active conformation was higher in rHDLs than in DDM micelles (Figure 3).

Although the transition time from inactive metarhodopsin I to active metarhodopsin II, as determined by visible spectroscopic analyses, is reportedly 6 ms,[13] there is no information available about the exchange rates between the active and inactive conformations of GPCR TM regions with diffusible ligands in physiologically relevant lipid-bilayer environments. Here, we reveal that the exchange rate between the inactive and active conformations of β_2AR in rHDLs were on the millisecond timescale (Figure 3). These equilibria on the millisecond timescale would likely be common to the class A GPCRs because the conformational changes in the TM region upon activation are broadly conserved.[4]

Our time-course simulation of G-protein signaling, based on the exchange rates of β_2AR when bound to a neutral antagonist or a weak partial agonist and the previously reported intracellular signaling reaction rates,[14] revealed that G-protein activation and the increase in cAMP were on timescales of hundreds of milliseconds and seconds, respectively (Figure S17). This is in agreement with experimentally observed cAMP increases within seconds[15] and the G-protein-coupled inward rectifier channel activations within hundreds of milliseconds.[16]

In the case of receptor tyrosine kinases (RTKs), which also mediate extracellular ligand-dependent cellular responses through multiple intracellular effectors, dimerization and subsequent tyrosine phosphorylation occur on the timescale of seconds to minutes,[17] thus making signaling from RTKs slower than GPCR signaling. The fast conformational change of GPCRs is a result of preformation of the active conformation, as exemplified by their basal activity, to enable rapid neurotransmission and sensory perception.

We developed a deuteration method for GPCRs expressed in an insect cell/baculovirus expression system, which increased the sensitivities of the methionine methyl resonances from β_2AR in rHDLs by 5-fold. Our NMR analyses revealed that the exchange rates in the conformational equilibrium of β_2AR in rHDLs were remarkably different from those for β_2AR in detergents. The fast timescales of the GPCR signaling, calculated from the exchange rates, enable rapid neurotransmission and sensory perception. These findings provide structural insights into GPCR signaling under physiological conditions.

Received: June 26, 2014
Revised: August 13, 2014
Published online: October 3, 2014

Keywords: G-protein-coupled receptors · isotopic labeling · lipid bilayers · membrane proteins · NMR spectroscopy

[1] M. Rask-Andersen, M. Almen, H. Schiöth, *Nat. Rev. Drug Discovery* **2011**, *10*, 579 – 590.
[2] Y. Kofuku, T. Ueda, J. Okude, Y. Shiraishi, K. Kondo, M. Maeda, H. Tsujishita, I. Shimada, *Nat. Commun.* **2012**, *3*, 1045.
[3] T. H. Kim, K. Y. Chung, A. Manglik, A. L. Hansen, R. O. Dror, T. J. Mildorf, D. E. Shaw, B. K. Kobilka, R. S. Prosser, *J. Am. Chem. Soc.* **2013**, *135*, 9465 – 9474; R. Nygaard, Y. Zou, R. O. Dror, T. J. Mildorf, D. H. Arlow, A. Manglik, A. C. Pan, C. W. Liu, J. J. Fung, M. P. Bokoch, F. S. Thian, T. S. Kobilka, D. E. Shaw, L. Mueller, R. S. Prosser, B. K. Kobilka, *Cell* **2013**, *152*, 532 – 542; J. J. Liu, R. Horst, V. Katritch, R. C. Stevens, K. Wüthrich, *Science* **2012**, *335*, 1106 – 1110; R. Horst, J. J. Liu, R. C. Stevens, K. Wüthrich, *Angew. Chem. Int. Ed.* **2013**, *52*, 10762 – 10765; *Angew. Chem.* **2013**, *125*, 10962 – 10965.
[4] X. Deupi, J. Standfuss, *Curr. Opin. Struct. Biol.* **2011**, *21*, 541 – 551.
[5] T. H. Bayburt, Y. V. Grinkova, S. G. Sligar, *Nano Lett.* **2002**, *2*, 853 – 856; A. Nath, W. M. Atkins, S. G. Sligar, *Biochemistry* **2007**, *46*, 2059 – 2069; M. R. Whorton, M. P. Bokoch, S. G. F. Rasmussen, B. Huang, R. N. Zare, B. Kobilka, R. K. Sunahara, *Proc. Natl. Acad. Sci. USA* **2007**, *104*, 7682 – 7687; C. Yoshiura, Y. Kofuku, T. Ueda, Y. Mase, M. Yokogawa, M. Osawa, Y. Terashima, K. Matsushima, I. Shimada, *J. Am. Chem. Soc.* **2010**, *132*, 6768 – 6777.
[6] S. Imai, M. Osawa, K. Mita, S. Toyonaga, A. Machiyama, T. Ueda, K. Takeuchi, S. Oiki, I. Shimada, *J. Biol. Chem.* **2012**, *287*, 39634 – 39641.
[7] M. Etzkorn, T. Raschle, F. Hagn, V. Gelev, A. J. Rice, T. Walz, G. Wagner, *Structure* **2013**, *21*, 394 – 401; F. Hagn, M. Etzkorn, T. Raschle, G. Wagner, *J. Am. Chem. Soc.* **2013**, *135*, 1919 – 1925; T. Raschle, S. Hiller, T.-Y. Yu, A. J. Rice, T. Walz, G. Wagner, *J. Am. Chem. Soc.* **2009**, *131*, 17777 – 17779.
[8] A. D. Gossert, A. Hinniger, S. Gutmann, W. Jahnke, A. Strauss, C. Fernandez, *J. Biomol. NMR* **2011**, *51*, 449 – 456.
[9] D. R. O'Reilly, L. K. Miller, V. A. Luckow, *Baculovirus Expression Vectors*: *a Laboratory Manual*, Oxford University Press, Oxford, **1992**.
[10] S. Kubo, N. Nishida, Y. Udagawa, O. Takarada, S. Ogino, I. Shimada, *Angew. Chem. Int. Ed.* **2013**, *52*, 1208 – 1211; *Angew. Chem.* **2013**, *125*, 1246 – 1249.
[11] V. Cherezov, D. M. Rosenbaum, M. A. Hanson, S. G. F. Rasmussen, F. S. Thian, T. S. Kobilka, H.-J. Choi, P. Kuhn, W. I. Weis, B. K. Kobilka, R. C. Stevens, *Science* **2007**, *318*, 1258 – 1265; D. M. Rosenbaum, V. Cherezov, M. A. Hanson, S. G. F. Rasmussen, F. S. Thian, T. S. Kobilka, H.-J. Choi, X.-J. Yao, W. I. Weis, R. C. Stevens, B. K. Kobilka, *Science* **2007**, *318*, 1266 – 1273.
[12] S. G. F. Rasmussen, B. T. DeVree, Y. Zou, A. C. Kruse, K. Y. Chung, T. S. Kobilka, F. S. Thian, P. S. Chae, E. Pardon, D. Calinski, J. M. Mathiesen, S. T. A. Shah, J. A. Lyons, M. Caffrey, S. H. Gellman, J. Steyaert, G. Skiniotis, W. I. Weis, R. K. Sunahara, B. K. Kobilka, *Nature* **2011**, *477*, 549 – 555.
[13] Y. Shichida, H. Imai, *Cell. Mol. Life Sci.* **1998**, *54*, 1299 – 1315.
[14] J. J. Saucerman, L. L. Brunton, A. P. Michailova, A. D. McCulloch, *J. Biol. Chem.* **2003**, *278*, 47997 – 48003.
[15] J. Leroy, A. Abi-Gerges, V. O. Nikolaev, W. Richter, P. Lechene, J.-L. Mazet, M. Conti, R. Fischmeister, G. Vandecasteele, *Circ. Res.* **2008**, *102*, 1091 – 1100.
[16] M. Bunemann, M. M. Bucheler, M. Philipp, M. J. Lohse, L. Hein, *J. Biol. Chem.* **2001**, *276*, 47512 – 47517.
[17] B. N. Kholodenko, *Nat. Rev. Mol. Cell Biol.* **2006**, *7*, 165 – 176; J. L. Swift, A. G. Godin, K. Dore, L. Freland, N. Bouchard, C. Nimmo, M. Sergeev, Y. De Koninck, P. W. Wiseman, J.-M. Beaulieu, *Proc. Natl. Acad. Sci. USA* **2011**, *108*, 7016 – 7021.

